An experimental study of an ejector-boosted transcritical R744 refrigeration system including an exergy analysis

Anas F A Elbarghthi, Armin Hafner, Krzysztof Banasiak, Vaclav Dvorak

Corresponding author

Anas F A Elbarghthi

Department of Applied Mechanics, Technical University of Liberec

Studentská 1402/2, 46117 Liberec, Czech Republic

Email: anas.elbarghthi@tul.cz

Author:

Armin Hafner

NTNU Department of Energy and Process Engineering,

Kolbjørn Hejes vei 1d, 7465 Trondheim, Norway

Author:

Krzysztof Banasiak

SINTEF Energy Research

7465 Trondheim, Norway

Author:

Václav Dvořák

Department of Applied Mechanics, Technical University of Liberec

Studentská 1402/2, 46117 Liberec, Czech Republic

Abstract:

The field of refrigeration witness a massive transition in the supermarket with a strong focus reflected on energy consumption. The use of ejector allows for overcoming the significant exergy destruction lays on the expansion processes of the cooling systems and led to spark improvement in the system performance by recovering some of the expansion work. In this study, a detailed experimental work and exergy analysis on the R744 transcritical ejector cooling system was investigated. The experiment was implemented on the commercial ejector cartridge type (032F7045 CTM ELP60 by Danfoss). The impact of different operating conditions determined by exit gas cooler pressure and temperature, evaporation temperature and receiver pressure was examined. The ejector performance of the pressure lift, mass entrainment ratio, work rate recovery and efficiency were evaluated. In addition, exergy efficiency and the variation of exergy produced, consumed, and destruction were assessed based on the transiting exergy. The result revealed better overall performance when the ejector operated at transcritical conditions. The ejector was able to recover up to 36.9% of the available work rate and provide a maximum pressure lift of 9.51 bar. Moreover, it was found out that the overall available work recovery potential increased by rising the gas cooler pressure. Out of the findings, the ejector could deliver maximum exergy efficiency of 23% when working at higher motive nozzle flow temperatures along with providing lower exergy destruction. The experiment results show that the amount of the exergy consumed and destruction were gradually increased with higher gas cooler pressure and, in contrast, decreasing with higher motive nozzle flow temperature.

Nomenclature

Abbreviations

COP	Coefficient of performance
HFC	Hydrofluorocarbon
HFOs	Hydrofluoroolefins
HP	High pressure
HPV	High pressure valve
LEJ	Liquid ejector
LP	Low pressure
MFM	Mass flow meter

VEJ	Vapour ejector	

Units and Symbols

e	Specific exergy	(kJ/kg)
$\dot{E}$	Exergy rate	(kW)
ER	Mass Entrainment Ratio	(-)
h	Specific enthalpy	(kJ/kg)
$\dot{m}$	Mass flow rate	(kg/s)
P	Pressure	(bar)
s	Specific entropy	(kJ/kg.K)
T	Temperature	(°C)
u	Axial velocity	(m/s)
$\dot{W}$	Work rate	(kW)
x	Mass fraction	(-)

Greek symbols

β	Coefficient of liquid mass balance
∇	Consumed
Δ	Produced
η	Efficiency

Subscripts

eje	Ejector
evap	Evaporation
in	Inlet of component
MN	Motive nozzle
o	dead state
out	Outlet of component
rec	Receiver pressure
recv	Recovery
SN	Suction nozzle
tr	Transiting

1. Introduction

Owing to the increasing levels of parameters influencing global warming, potential ozone depletion refrigerants have been replaced by eco-friendly and neutral impact alternatives such as the natural working fluid CO_2 (denoted as R744) [1,2]. The properties of CO_2 have made the R744 systems to be cost-effective and efficient. This is based on the thermophysical advantages that CO_2 offers; such as high thermal conductivity, high vapor density, and low viscosity. Additionally, CO_2 has an A1 safety classification based on ASHRAE. It is also an odourless and colourless gas with a slightly pungent taste of acid as well as being non-flammable and non-toxic [3]. Based on the exceptional characteristics of CO_2 as a refrigerant, it is currently being used in the development of refrigeration and heat pumps, such as booster systems for commercial applications [4].

The major exergy destruction in commercial CO_2 systems lies in the expansion of the gas during the throttling process. The throttling losses have led to a sparked interest in developing new techniques on the recovery and reduction of expansion work and, consequently the increase in the overall performance of the system [5, 6]. In contrast, the two-phase ejector used in commercial booster systems to regain those significant irreversibilities associated with the expansion valve. Recently, two-phase ejectors have gained massive popularity with their simplicity leading to enhance the energy efficiency of the cooling systems [7].

In the course of eliminating refrigerants with high potential for global warming, an auxiliary compressor was incorporated into the conventional CO_2 system with an upstream throttle valve of the fluid collector. This resulted in a significant drop in the rate of destruction of exergy through parallel compression. Nonetheless, in R744 booster configuration with parallel compression, recovering some potential work to improve the energy performance further can be achieved by replacing the main valve with an ejector [8]. In this case, the ejector by its application under isentropic conditions entrains the low-pressure stream with a motive stream of high pressure and consequently reducing the energy losses partly. The kinetic energy exchange to pressure energy during entrainment raises the pressure of both streams at the outlet. Using this method is not only effective in increasing energy performance by reducing the pressure ratio within the compressor section but also contributes to a higher coefficient of performance (COP) of the overall system as compared to other configurations without the ejector [9, 10]. The refrigeration of the supermarket system employs this method to reduce electric power consumption next to increased energy performance primarily due to reduced compressor work.

The advantages of applying a single ejector for expansion in refrigeration systems design with optimization of operating

conditions have been explored widely in several experimental approaches to reveal an 8 – 27% increase in COP. For example, in an experiment performed by Elbel [11] the results showed significant benefits of using a transcritical ejector system to overcome large losses occurring due to throttling. COP and cooling capacity were simultaneously increased for a range of test conditions of internal heat exchanger up to 7% and 8%, respectively. Additionally, Lucas et al. [12] investigated the maximum COP of the refrigeration system of both expansion valve and ejector cycles without an internal heat exchanger. Their COP was observed to reach a 17% improvement over the expansion valve cycle. However, the performance of the two-phase ejector equipped systems was found not only to be sensitive to the efficiencies of the individual geometries but also to operating conditions. On this account, He et al. [13] tracked the dynamic responses of a transcritical CO_2 ejector refrigeration system to predict the ejector efficiency and system performance with a virtual online cascade controller. The controller tracks the optimal pressure of the gas cooler and analyses the performance based on the control of the variable area of the nozzle throat, which verified an increase to optimal performance with the tracker incorporated. Nonetheless, the working condition for optimal performance does not indicate a maximum ejector cooling capacity or efficiency in simulation. However, the system performance was improved in the experimental system using the controller, although great variations in performance occur for different operating conditions. For a variable compressor speed, a multivariable controller according to studies is necessary to drive an increase in performance in the transcritical state of the ejector. This concept was simulated by Yang et al. [14] on the R744 refrigeration system equipped with a controllable ejector and was verified for improving the energy performance by predicting the optimal gas cooler pressure. In a study on the R744 multi-ejector supermarket refrigeration system by Hafner et al.[15], a single stage and multi-ejector system with flash gas bypass and heat recovery was analyzed for four days in three different European countries. The systems, equipped with a controllable ejector was assessed for different fixed geometries. The results depicted a 30% increase in the energy performance of the multi-ejector setup over the reference booster system. Recovery of work of potential work with ejectors has been addressed and proven in several studies to significantly increase the COP of cooling and heating modes in supermarket refrigeration and heat recovery systems.

An additional configuration setup to enhance the performance of the parallel-compression R744 system is to replace the high-pressure expansion valve with a block of parallel ejectors to sustain the discharge pressure through a discrete opening feature. This study was performed by Banasiak et al. [16] with a thoroughly designed and experimentally verified four different cartridge multi-ejector pack. In the test, the performance of the individual cartridge is assessed. The whole ejector pack was evaluated for the possibility of maintaining the discharge pressure as the main expansion component, as well as its improvement of COP. The results depicted higher individual ejector efficiencies with an overall improvement in energy

performance. The multi-ejector pack was also verified to work efficiently in adapting and retaining precise discharge pressure under variable loads, even with a simple controlling method. Although the estimation method used to evaluate the COP and exergy efficiencies yielded results partly comparable to the real applications, increase up to 8%, and 13% of improvement was indicated. Based on the effect of the geometries and operating conditions on efficiency, several experimental works have been conducted in that focus [17]. In XU et al. [18], an adjustable ejector was used to change the nozzle throat area at a distributed ejector efficiency within the range of 20–30% to maximize the system COP by increasing high-side pressure. Each geometric configuration gives a potential solution on which performance can be assessed. Smolka et al. [19] studied the parallel arrangement of ejectors for both fixed and adjustable geometries to provide an incremental or flexible mass flow of refrigerant with different nozzle configurations. The approach was simulated for transcritical parameters at various sizes for each geometric concept. For a range of operating conditions considered, the fixed geometry ejector design produced high efficiencies, whereas the controllable geometry ejector design was limited to a 35% reduction in the throat area with a subsequent gradual decrease in efficiency when the throat is reduced further. Palacz et al. [20] optimized the shape of a CO_2 ejector by six geometry parameters which enhanced the ejector efficiency by 6%. Consequently, different operating conditions and geometries were experimentally studied by Liu et al. [21] to provide correlations between the motive and suction nozzle efficiency including the mixing section efficiency. Elbel and Hrnjak [22] showed in their experimental result that COP could be increased up to 7% over a conventional system with the incorporation of the ejector and also reported an improvement in static pressure recovery with a small angle of 5° diffuser design. Nakagawa et al. [23] studied how the mixing length altered the ejector performance in the cycle and concluded that COP could be lowered by 10% for improper sizing of the length of the mixing chamber as compared to conventional systems. The low critical temperature of R744 allows the system to operate in a transcritical state, however, this lowers the thermodynamic system performance compared to the subcritical condition based on the higher rates of exergy destruction from throttling the supercritical state to the subcritical [6]. Therefore, to spread its use, exergy performance, and exergy destruction and efficiencies should be evaluated. Recent investigations use a CO_2 two-phase ejector analysis of exergy to obtain how ejector irreversibilities are affected by different operating conditions [24–26]. Boccardi et al. [27] reported a reduction of the throttling irreversibilities losses by 46% using multi-ejector for expansion with a maximum increase in exergy efficiency by 9%. Ersoy et al. [28] provided analytical study focused on the performance of the transcritical CO_2 ejector cooling cycle. The results showed the possibilities of 39.1% ejector irreversibility decrease compared to the classic refrigeration cycle and 5.46% lower associated with turbine expander systems.

In general, the transcritical CO_2 refrigeration system exhibits relatively high exergy destruction. The overall exergy destruction can be reduced by 43.44% when system components, specifically the compressor which contribute to the largest destruction of exergy followed by the ejector, evaporator, and gas coolers [26]. Taslimi et al. [29] studied different transcritical CO_2 ejector systems at similar cooling capacity based on the laws of thermodynamics. The result illustrated that the evaporator exhibited major exergy destruction in the cycle by 33% followed by the compressor with 25.5% then the ejector at 24.4%. Fangtian and Yitai [30] concluded that utilizing ejector would decrease the exergy loss by 25% in a CO_2 transcritical cycle as compared to the conventional cycle. A current study by Gullo et al. [25] reported a 39% overall reduction of exergy destruction in multi-ejector supported CO_2 system compared to the conventional booster system. The thermodynamic efficiencies of the cooling cycles, heat pump systems, ventilation, and air conditioning are sensitive to the role of ejector operating conditions in real applications as clarified in detail previously. Due to the different cooling demands and ambient temperatures required to operate Supermarket CO_2 refrigeration systems with variations throughout the day, the ejector is required to operate efficiently over a wide range of ambient conditions. Consequently, this paper aimed to provide an extensive experimental study pointed at the low-pressure lift type ejector's performance mapping. The impact of different operation conditions on the behaviour of the ejector performance is introduced. The results are analyzed through a sensitivity analysis of different variables such as the gas cooler outlet conditions and evaporating temperature at different receiver pressure to account for the optimum working conditions. The ejector performance was measured in terms of entrainment ratio, pressure lift, ejector efficiency, and work rate recovery. To better understand the influence of the boundary conditions at which the ejector performs the best, the exergy distribution was investigated based on the transiting exergy concept. The result provided in this paper were obtained based on the collected experimental data, unlike different research papers using other theoretical models to predict the ejector performance.

2. The R744 multi-ejector module

2.1. Description of the multi-ejector pack

Carbon dioxide systems have been modified with the inclusion of multi-ejector systems to increase its efficiency as well as widen the range of applicability of the CO_2 technology. In these systems, a control strategy is imperative since R744 systems come mostly with high throttling losses to control the heat rejection accurately. The commercial multi-ejector block manufactured by Danfoss is composed of parallel arrangements of different geometry cartridges as depicted in Fig. 1. The desired ejector cartridge is activated by the ordinary coil (solenoid shut-off valves) located at the motive nozzle inlet. There

are built-in check valves in each ejector at the suction nozzle to regulate the flow with preventing back flow which can create pressure instability. The block has a discharge port for the mixed elevated pressure fluid and a low-pressure and high-pressure side suction ports for suction of entrained fluid and motive fluid, respectively. The side of each flow port (motive, suction, and discharge) is equipped with pressure sensors to measuring the pressure level in each port. The flow enters the multi-ejector through the strainer/filter in front of the high-pressure inlet which is placed in a separate port. However, there exists a high-pressure valve (HPV) which arranged in parallel to the block as a form of safety measures and contributed as a pressure regulator for the gas coolers. The multi-ejector block is implemented due to three major advantages. The first being the fact that, due to the pre-compression of CO_2 from the evaporator pressure level to an intermediate pressure, there is a significant reduction of compressor power input needed. Moreover, the refrigerating effect is highly increased with the refrigerant entering the evaporator at a much lower vapor quality. Lastly, the possibility of overfeeding of the evaporators increases the effectiveness of the overall heat exchange process. Consequently, the work can be reduced by elevating the evaporation pressure to higher suction pressure, hence reducing defrosting cycles demand in the evaporators. There are two kinds of ejectors based on the application; the low-pressure ejectors (LP) and the high-pressure ejectors (HP). The low-pressure ejectors are used for low lift applications such as pumping gas from the evaporators back to the receiver as well as ensuring low-pressure lift for suction mass flow. A high-pressure ejector system lifts the pressure of a liquid or vapor from the medium temperature suction level in a system with parallel compression. From the receiver, it then moves to the parallel compressor and the main purpose of this is to ensure high-pressure lift for lower suction mass flow. Relative to the low-pressure ejectors, flash formation is high and the system significantly benefits from pre-compression of the gas.
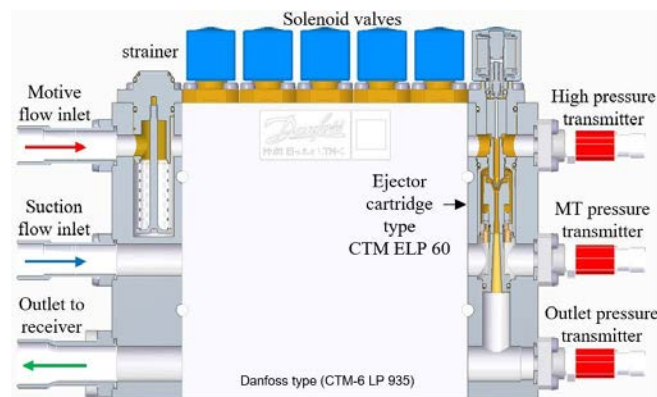

Figure 1: Sketch of the multi-ejector block used from Danfoss [31].

2.2. Ejector working principle

Two-phase ejectors have gradually replaced expansion devices in the traditional vapor compression systems as a result of the high reduction in compression work needed. Additionally, rather than isentropic expansion, an isenthalpic expansion (at constant enthalpy) which causes high throttling losses, is recovered. For these reasons, two-phase ejectors have attracted a lot of research in the scientific community. The ejector does not contain any moving parts and composes of the suction chamber, motive nozzle, diffuser and mixing chamber. Based on the two flow streams in the ejector, which are the entrained and the motive fluid flow, the basic working principle of this system is the conversion of pressure energy to kinetic energy isentropically. The driving force for the ejector is the primary fluid, which is usually termed as the motive fluid. The high-pressure primary fluid enters the converging-diverging nozzle and expansion occurs, causing an acceleration towards the motive nozzle. At this point, the pressure generated is very low accommodated with tangential force develops at the edge of the motive flow and a supersonic flow occurs at the exit. As a result, the pressure difference between the working fluid exiting the evaporator and the expanded refrigerant from the motive nozzle causes the suction fluid to be sucked toward the mixing chamber with higher velocity. The entrained fluid is accelerated by the high-velocity motive fluid in the mixing section. The mixing chamber is composed of a constant cross-section part and a pre-mixing section. Here, the two flow streams start mixing, and there is a transmission of energy of the primary fluid in the form of kinetic energy to the entrained fluid (to increase its velocity), and part of the energy converted to pressure energy, whereas some of the energy dissipated as heat due to the mixing and friction. The shock train phenomena also occur in the mixing chamber region, where oblique shock wave sand expansion occur and diminish until they disappear. This is primarily caused by the suction and motive nozzle outlet pressure difference. Due to this momentum exchange, the mixed fluid is forced downstream. Furthermore, it is imperative for the mixing chamber section to have a specified length to prevent reverse flow [32]. As the mixed fluid enters the diffuser section, the pressure of the fluid begins to increase right to the end of the diffuser. The pressure of the outlet mixed-flow lies between that of the entrained fluid and the motive nozzle flow pressure. The changes in velocity (deceleration) in this section convert kinetic energy back to potential energy to obtain a high net pressure for the mixed fluid flow.

3. Experiment setup and analysis method

3.1. Test facility layout

Vapour compression unit design and controlling strategy were described in detail by Banasiak et al. [16]. The multi-ejector pack was installed at the NTNU/SINTEF energy research laboratory in Trondheim-Norway and presented for vapor ejectors

experiment. The test rig is represented in Fig. 2. The facility consisted of a refrigerant circuit using R744 as the refrigerant and a glycol cycle which integrated to serve as a gas cooler heat sink and the evaporator heat source. The simplified R744 compression test rig is illustrated in Fig. 3. Additionally, the auxiliary cooling water network was utilized to provide the cooling media for the second stage gas cooler. The refrigerant loop of the multi-ejector test rig contains Mt based load compressor type (Dorin CD1400H) and two other parallel compressors type (Dorin CD380H and Dorin CD1000H) to inverters for continuous work regulation. The unit has six different heat exchangers working as following; type (SWEP B18Hx100) heat exchanger serves as the 1st stage gas cooler, type (Kaori K095C-30C- NP8M) heat exchanger for both peak-load evaporator and 2nd stage gas cooler, type (SWEPB16DWHx100) for the base-load evaporator and two internal heat exchangers connected to the house glycol/water supply system. The gas coolers control the outlet temperature of the refrigerant by absorbing heat using the glycol loops while the internal heat exchangers utilized to set the subcooling degree as protecting the compressors of having any liquid droplets at the suction line. The system supplied by appropriate oil management consists of an oil separator and an oil reservoir with several solenoid valves connecting the oil separators to the reservoir and feed the returning oil to the compressors. The system contains three electronic expansion valves manufactured by Danfoss. There is a high-pressure valve HPV type (CCMT8) to decrease the outlet gas cooler pressure to an intermediate pressure level of the liquid receiver, whereas the other two work as metering valves at evaporators type (CCM20). There are 50-L pressure tanks liquid receiver and separator provided with liquid level indicators. The facility data acquisition system was supplied with Danfoss AKS 21 APT1000 temperature sensors, pressure transmitters and calibrated Coriolis type of mass flow meters (RHEONIK RHM06for refrigerant circuit and RHEONIK RHM15 for glycol circuit). The instrumentation accuracy and their data range are listed in Table 1. The uncertainty analysis accompanied the measurements to justify the quality and reliability of the experimental results and the derived quantities. The propagation of uncertainty method used to reflect the error distribution of these indirectly measured variables calculated based on Guide to the Expression of Uncertainty in Measurement [33]. The uncertainties mean values were registered as follows: ±0.3 bar for pressure measurements, ±0.18 K for temperature measurements, ±0.27 for the COP, ±7.5 × 10^{-5} kg.s^{-1} for the mass flow rate measurements, ±3.1 × 10^{-3} for entrainment ratio, ±6.9 × 10^{-3} for the ejector efficiency, ±3.1 × 10^{-5} kW for the work recovery rate and ±8.2 × 10^{-4} kW for the overall available work recovery potential.

The test rig was equipped with a multi-ejector pack type (CTM-6 LP 935) manufactured by Danfoss and containing a series of parallel ejector cartridges. There are shut-off valves (solenoid valves) installed on every cartridge that allows for control the motive nozzle individually to supply to the high-pressure flow. This experimental work was performed using the ejector

cartridge (VEJ1) type (032F7045 CTM ELP 60) which has not been studied before as the case study. The main cartridge geometries are shown in Table 2.
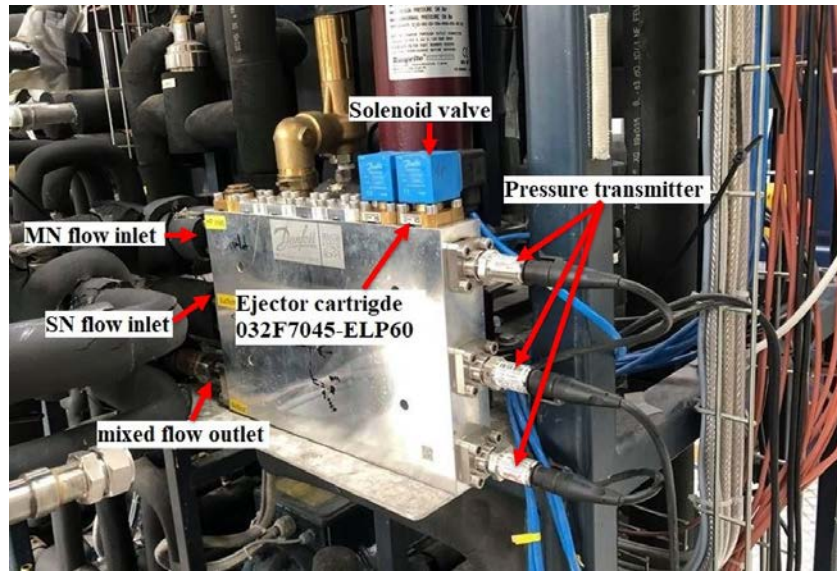

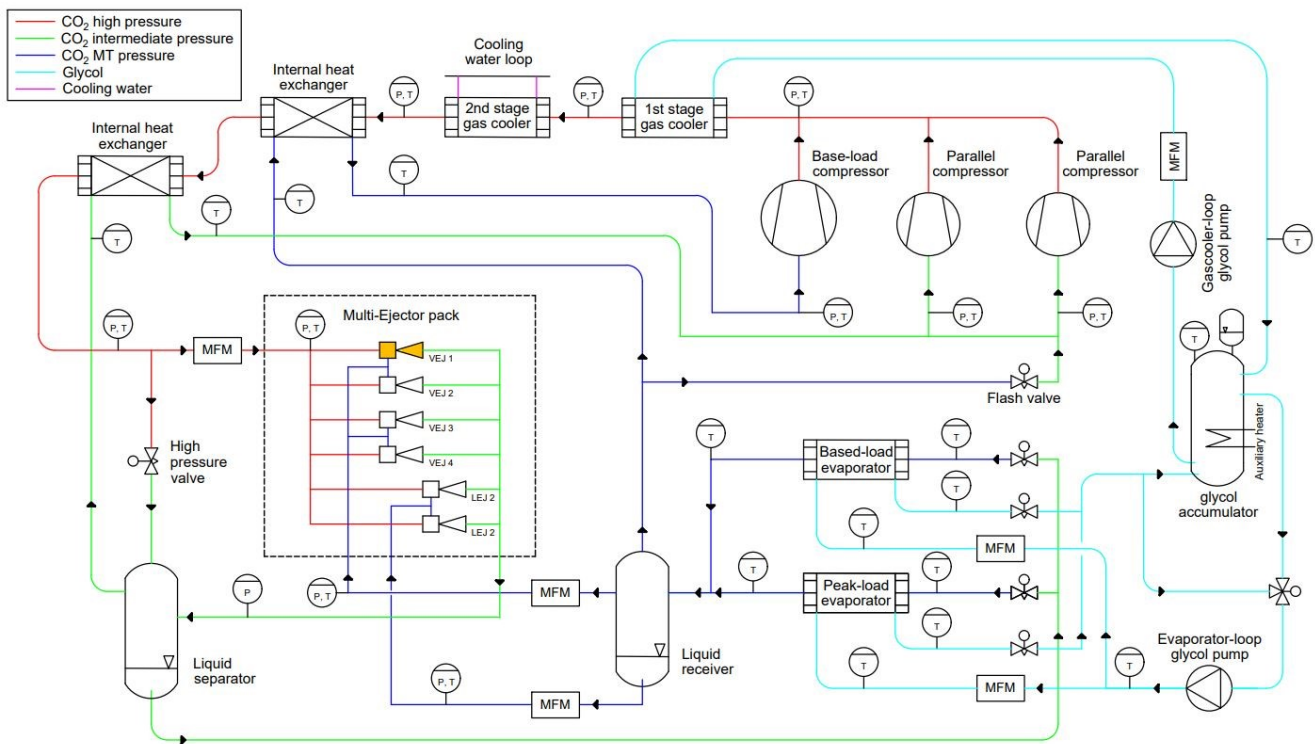Figure 2: The test rig equipped with a multi-ejector pack.

Figure 3: Simplified process and instrumentation diagram of the experimental test facility, including the R744 refrigerant and the glycol loop.

Table 1

The set of the instrumentations used for experimental investigation

Measured quantity	Instrument	Data range	Accuracy
Temperature	Resistance thermometer PT1000	-70°C÷180°C	±(0.3 + 0.005 t), T in °C
Mass flow rate	Coriolis-type RHM06	0÷20 kg min^{-1}	±0.2% of reading
Mass flow rate	Coriolis-type RHM15	0÷200 kg min^{-1}	±0.2% of reading
Pressure	Piezoelectric transmitter	0÷150 bar	±0.3% of reading
Electric power consumption	Inverter IP55 Type 12	0÷20 kW	±0.05kW

Table 2

Ejector cartridge CTM ELP 60 main geometry parameters installed in the R744 multi-ejector [31].

Parameter name	Unit	Value
Motive nozzle inlet diameter	mm	3.8
Motive nozzle throat diameter	mm	0.71
Motive nozzle outlet diameter	mm	0.78
Motive nozzle converging angle	degree	30
Motive nozzle diverging angle	degree	2
Diffuser diameter	mm	7.3
Diffuser angle	degree	5

HPV was running in parallel with the ejector to secure having an accurate high-pressure level during the system operation. The ejector and HPV are contributed to control the liquid receiver pressure level by changing the HPV opening degree and determine the multi-ejector block capacity. The ejector inlet port for the motive flow stream is connected to the gas cooler outlet through the mass flow meter. Both ejector vapor and liquid suction are provided with a separate mass flow meter aiding to monitor the flow into the ejector from the liquid separator located downstream. The ejector discharged the outlet mixed flow into the liquid receiver, where the vapor was separated and compressed by the parallel compressors whiles the liquid portion fed back the evaporators through the expansion valves then recirculating the refrigerant to the

liquid separator. The system consists of different pressure levels described in Fig. 3 in different colors. CO_2 loop consists of a high-pressure level (red lines), which varies from 110 to 50 bar from the compressor discharge to the HPV and ejector motive nozzle, then the refrigerant will be throttled to the intermediate pressure level from 50 to 30 bar (green lines) and passed to the liquid separator. The liquid port in the receiver supplied the evaporators with the required CO_2 through the connected thermal expansion valves while the receiver vapor port connected with the parallel compressors suction line. The throttled refrigerant from the evaporators flows to the liquid receiver, which is represented as the low pressure level (MT pressure) at 25 to 30 bar (blue lines) where the liquid separation takes place and fluid recirculated to the ejector suction manifold and base-load compressor. The ejector performance is controlled by the receiver pressure level which representing the ejector discharge mixed-flow pressure and the inlet pressure and temperature of the motive and suction nozzle flow streams. The system was designed to control and maintain all the required boundary conditions flexibly by following different procedures. For example, it adjusts the inlet coolant water mass flow rate in the gas cooler to control the motive nozzle flow temperature. Similarly, it controls the receiver pressure by regulating the opening degree of the flash gas valve, etc.

3.2. Ejector performance characteristics

The performance of the two-phase ejector, used for expansion work recovery in the refrigeration cycles, is commonly analyzed by several parameters. The main significant factors considered to evaluate the ejector are the pressure lift (P_{lift}), mass entrainment ratio (ER), ejector compression ratio, and the expansion work recovery, which is usually termed as the ejector efficiency (η_{eje}). The pressure lift represents the amount of pressure difference between the ejector discharged mixed-flow (P_{rec}) and suction nozzle flow (P_{SN}). In this low-pressure ejector (LP), the refrigerant is being pumped from the evaporator back to the receiver and ensure relatively low pressure lift at a high suction nozzle mass flow rate. The mass entrainment ratio is determined as the ratio between the suction and the motive nozzle mass flow rates, as shown in equation (2). This ratio assesses the capability of the ejector to entrain the refrigerant from the evaporator through the liquid separator back to the liquid receiver. Normally, the ejector ought to ensure large suction mass flow besides delivering a large pressure lift to obtain a good ejector performance.

$$P_{lift} = P_{rec} - P_{SN} \tag{1}$$

$$ER = \dot{m}_{SN}/\dot{m}_{MN} \tag{2}$$

In fact, the ejector has two choking phenomena that impact the general performance. The first choking exists at the motive nozzle and the second occurs throughout the entrained flow. The ejector performance itself is divided into three operational modes according to the outlet mixed flow, critical, subcritical and backflow mode termed as double-choking, single choking, and malfunction mode respectively. At the critical mode operation, the mass entrainment ratio reaches the maximum and remains constant with a further decrease in the range of the ejector discharge flow pressure (receiver pressure) whereas both motive and suction nozzle flows are choked. In sub-critical mode, only the motive flow is choked because the receiver pressure increases higher than the ejector critical pressure value which results in decreasing the mass entrainment ratio. If the receiver pressure continues to rise, the ejector experiences a backflow where the suction nozzle flow stream reverses observed and the entrainment ratio ends up as lower than zero. This operation mode also called stall condition and occurred as a result of the ejector being forced to give a pressure lift that is relatively higher than what was designed for. Therefore, the motive flow utilized for pressure recovery will not be able to drive the entrained flow and the ejector will operate as a throttling valve only. The ratio between the ejector outlet pressure (P_{rec}) to the suction nozzle pressure (P_{SN}) is defined as the ejector compression ratio. It is also known as a pressure lift ratio or suction pressure ratio through the literature. The ejector efficiency is expressed in equation (3). It compares the overall available work recovery potential ($\dot{W}_{recv,max}$) based on the expansion work rate recovered by the ejector ($\dot{W}_{recv}$) [22]. The formula can be interpreted as the amount of the total power applied to compress the entrained flow isentropically to the ejector outlet over the maximum theoretical work recovery potential. Additionally, the ejector efficiency is used as a universally accepted approach to assess the overall ejector energy performance by reflecting the total irreversibility that occurs inside the ejector passages [34]. The efficiency can simply be calculated using the measured boundary operation conditions. From the formula, the receiver pressure (indicated as the ejector outlet pressure) plays a vital rule in controlling the ejector efficiency, and this will be evaluated within the scope of this paper.

$$\eta_{eje} = \frac{\dot{W}_{recv}}{\dot{W}_{recv,max}} = ER \frac{h(P_{eje,out}, \ s_{SN}) - h_{SN}}{h_{MN} - h(P_{eje,out}, \ s_{MN})} \tag{3}$$

4. Exergy analysis method

To detect the location and magnitude of irreversible losses in energy conversion system, several methods are used of which exergy analysis is the common method. This method detects losses in several ways. In the conventional way, although irreversibility can be detected, the nature of influence of individual components on each other in the system is not known as well as the possibility of eliminating individual inefficiencies. However, the advanced exergy model provides a

comprehensive information on exergetic performance of the system. The model quantitatively evaluates the interaction between the system components to determine the real system potential. The advanced exergy analysis is established based on the exergy destruction within a system based of constraints such as the system component under study and interaction with other components, manufacturing methods used and material costs and their influence on each other [25,26]. In this study, a concept initially proposed by Brodyansky et al. [35] is considered. This method analyses the transiting exergy of the two-phase ejector to evaluate the ejector exergy efficiencies under different operating conditions. The transiting exergy of the material stream which is the lowest exergy value is characterized by the intensive parameters of the inlet and outlet parameters of the system or defined by the parts of the system originally not included in the traditional approaches since it tends to include the effect of exergy variations caused by different factors which has the possibility of influencing changes in any thermodynamic system. As a result of this approach, exergy consumed and produced can be unequivocally defined. Using this approach, the different pressure of the receiver from exergy destruction and efficiencies can be obtained to evaluate the performance under different working conditions of different motive pressure and temperatures as well as to characterize the behaviour of three thermodynamic metrics that is, exergy produced, exergy consumed, and exergy destruction. The transiting exergy efficiency used for the evaluation of a two-phase ejector defined as follows;

$$\eta_{\text{eje,tr}} = \frac{\text{Exergy produced}}{\text{Exergy consumed}} = \frac{\Delta \dot{E}_{\text{tr}}}{\nabla \dot{E}_{\text{tr}}} \tag{4}$$

The exergy produced is the difference between the exergy flow rate at the outlet $\dot{E}_{\text{out}}$ and the transiting exergy $\dot{E}_{\text{tr}}$ as the lowest exergy value of a material stream, which is defined by the pressure and temperature at the inlet and outlet of a system along with the dead state temperature T_o (i.e., selected outdoor temperature). T_o was fixed to 20°C for the exergy calculation. It is worth stating that the results associated with an exergy analysis are not substantially affected by the adopted dead state [36]. It is also assumed that the minimum velocity is equal to zero. The exergy consumed is the difference between the inlet exergy flow rate $\dot{E}_{\text{in}}$ and the transiting exergy $\dot{E}_{\text{tr}}$. The exergy destruction or losses represent the difference between the exergy production and consumed or between the inlet and the outlet exergies $\dot{E}_{\text{tr}}$ and the specific exergy at state ($_i$) are calculated as follows:

$$e_i(P, T) = [h_i - h_o] - T_O(s_i - s_o) \tag{5}$$

$$\text{if } (T_{\text{in}} > T_o \text{ and } T_{\text{out}} > T_o): \dot{E}_{\text{tr}} = \dot{E}(P_{\min}, T_{\min}, u_{\min}) \tag{6}$$

$$\text{if } (T_{\text{in}} < T_o \text{ and } T_{\text{out}} < T_o): \dot{E}_{\text{tr}} = \dot{E}(P_{\min}, T_{\max}, u_{\min}) \tag{7}$$

$$\text{if } (T_{in} > T_o \text{ and } T_{out} < T_o) \text{ or } (T_{in} < T_o \text{ and } T_{out} > T_o) : \dot{E}_{tr} = \dot{E}(P_{min}, T_o, u_{min}) \tag{8}$$

$$\Delta\dot{E}_{tr} = \dot{m}_{MN}[e(P_{rec}, T_{rec}) - e(P_{rec}, T_o)] + \dot{m}_{SN}[e(P_{rec}, T_{rec}) - e(P_{SN}, T_{rec})] \tag{9}$$

$$\nabla\dot{E}_{tr} = \dot{m}_{MN}[e(P_{MN}, T_{MN}) - e(P_{rec}, T_o)] + \dot{m}_{SN}[e(P_{SN}, T_{SN}) - e(P_{SN}, T_{rec})] \tag{10}$$

The total exergies consumed and produced are linked with the motive and suction nozzle flow streams. The exergy production described by equation (9) emphasizes the increase of the specific thermal exergy. The temperature of the motive flow drops to the ejector outlet temperature caused by constant pressure addition at the mixing section. Likewise, the exergy of the suction fluid also increases towards the ejector outlet due the same constant pressure addition. Furthermore, the first term in the exergy consumption shown in equation (10) characterizes the decrease in the specific thermo-mechanical exergy of the motive fluid due to expansion and temperature drop and the second term shows the decrease in the specific thermal exergy of the suction nozzle flow due to constant pressure and increase in temperature. Further details can be seen in Ref. [24]. For the exergy calculations, all the thermodynamic properties of CO_2 are generated by using the NIST REFPROP 10 database.

5. Results and discussion

The system is a comprehensive test rig with many experimental possibilities, involving testing a large range of conditions and system configurations. The experimental work was carried out to evaluate the two-phase flow ejector performance under various operating conditions. Fig. 4 represents the experimental operation points selected. The motive nozzle MN flow conditions for the working ejector are illustrated in Fig. 4(a). The ejector motive nozzle flow pressure was tested at 60, 70, 80, 90, and 100 bar, whereas the outlet temperatures of the gas cooler were varied for 20, 25, 30, and 35°C to evaluate the ejector at transcritical and subcritical regions. The evaporation temperatures were selected in terms of refrigeration application usage at -6°C and -3°C with ejector suction nozzle SN flow pressure between 29.5 and 32 bar, as shown in Fig. 4(b). The ejector outlet conditions were determined by the liquid receiver pressure and the vapor quality defined based on the energy balance for the motive and suction nozzle flow to the ejector outlet, as represented in Fig. 4(c). Overall, around 236 experimental tests have been conducted to form a qualitative test campaign related to the different receiver pressure and entrainment ratio tendency.

During the operation, if the liquid mass of the ejector outlet two-phase flow at the liquid receiver will be in balance, then the system is running at a steady-state condition. In that case, the measurement data could be collected and analyzed. For that reason, the coefficient of liquid mass balance in the liquid receiver (β) was determined by equation (11) to indicate

the ejector expansion system steady-state operation and show how the load at the heat exchangers is stable [37]. This coefficient depends on the ejector mass entrainment ratio and the liquid fraction of the ejector outlet flow. If the coefficient value is situated close to zero, then the system is running at its ideal state and thus, the steady-state condition has been reached.
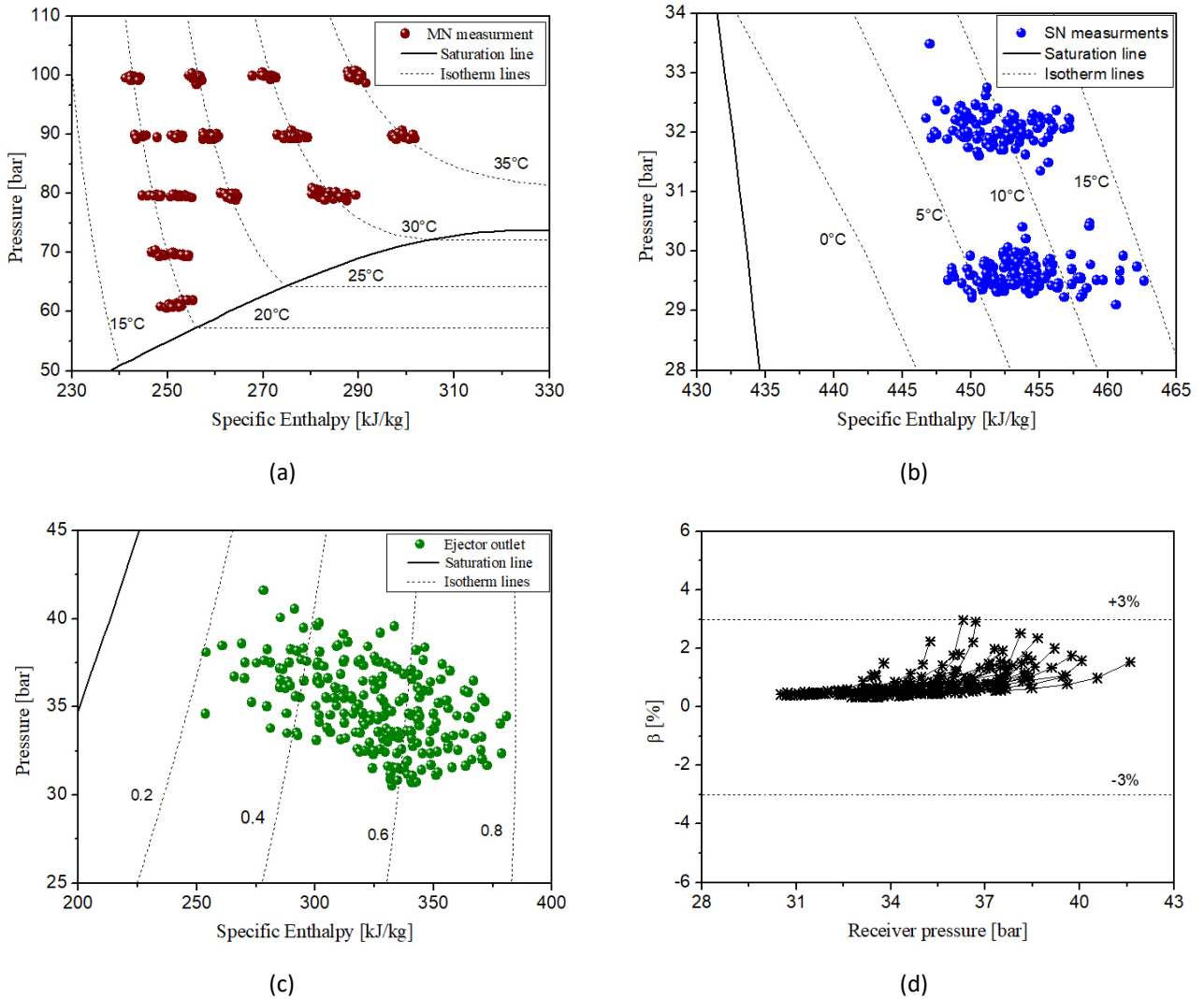

(a)

(b)

(c)

(d)

Figure 4: R744 ejector overall conducted experiments, (a) p-h diagram representing MN flow inlet conditions, (b) p-h diagram representing SN flow inlet conditions, (c) p-h diagram representing the outlet mixed flow to the receiver, (d) the calculated coefficient of liquid mass balance for different receiver pressure.

$$\beta = x_{rec} + \frac{x_{rec}}{ER} - 1 \tag{11}$$

The result in Fig. 4(d) indicates that the ejector was running under steady-state conditions and the coefficient of liquid mass balance rises with higher receiver pressure because of the mass entrainment ratio decreasing which resulting in less liquid mass flow out of the receiver comparing to the liquid mass flow from the ejector exit. This result might be similar

when comparing the coefficient of liquid mass balance at higher motive nozzle flow pressure because the specific enthalpy of the motive flow CO_2 will decrease and the mass fraction at the ejector exit will be increased to obtain the similar trend.

5.1. Effect of the operation conditions

In this section, the ejector operating parameters such as pressure lift, mass entrainment ratio, ejector efficiency and work rate recovery will be discussed at different boundary conditions. In Fig. 5, a comparison between the maximum ejector pressure lift with different inlet motive nozzle flow conditions is illustrated for all the collected data. The results reveal the expected outcome based on the ejector theory. At higher motive pressure, the ejector performed higher pressure lift according to the high expansion work potential in the motive nozzle. Measuring different range of the motive nozzle flow temperature (the gas cooler outlet temperature) at low motive pressure was not possible due to the system functional limitation, but it can be noted that the lowest measured value for the pressure lift was 0.81 bar and the highest was 9.51 bar. Besides, the maximum pressure lift could be gained at P_{MN}= 60, 70, 80, 90, and 100 bar were 4.91, 5.57, 7.19, 8.98, and 9.51 bar, respectively. Based on the experimental result, the ejector maximum pressure lift could be predicted in terms of the gas cooler pressure with linear relation, as presented in Fig. 5.
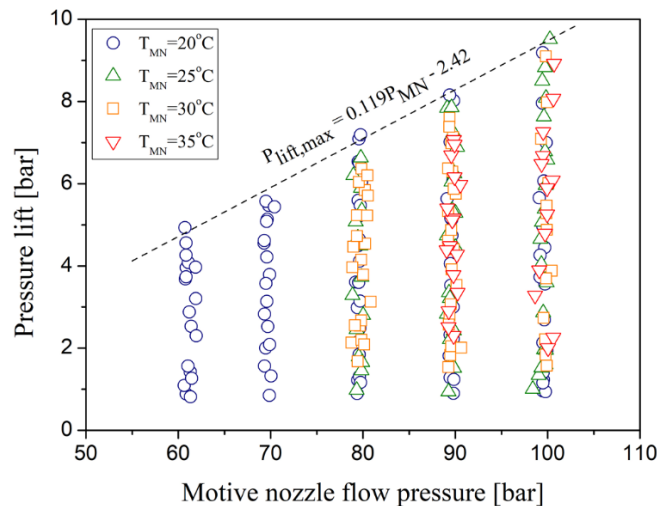

Figure 5: pressure lift as a function of motive nozzle inlet pressure.

The correlation could help in the controller system defining the highest possible ejector pressure lift, which indeed reduces the parallel compressor pressure ratio and plays a role in saving energy consumed and contribute to improving the system performance. The ejector efficiency proved an effective compression over the most working range conditions. Giving the result presented in Fig. 6, the ejector recorded the highest efficiency of 0.369 at P_{MN}=90 bar and T_{MN}= 25°C. These graphs were representing the best working region of the ejector efficiency at which the pressure lift of the ejector can be selected.

It can be noted that the points characterized by efficiency greater than 0.3 recognized at substantial P_{lift} from 2.4 to 8.2 bar. Moreover, increasing the motive nozzle flow pressure or temperatures will shift the working ejector efficiency peak to be at a higher pressure lift and extend the region of the high efficiency where the ejector can operate; for example, at P_{MN}=70 bar, the ejector could work with reasonable efficiency higher than 0.1 with pressure lift from 0.8 to 5.6 bar whereas at P_{MN}=100 bar the range is extended to P_{lift}=9.5 bar.
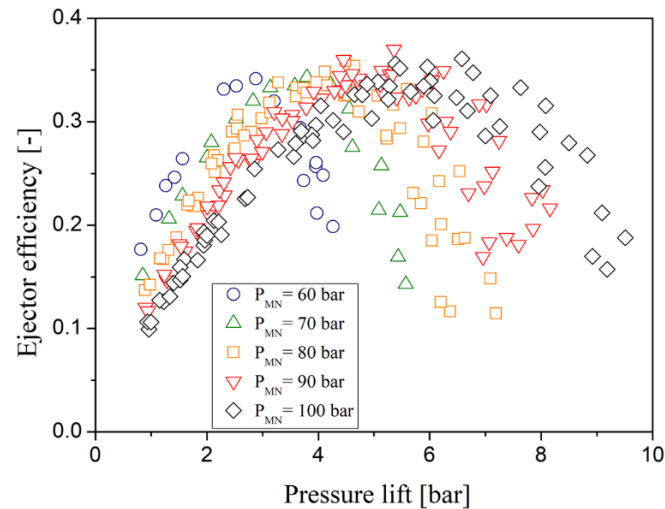
Figure 6: variation of ejector efficiency with pressure lift at different MN pressure.

Compared to the previous study, the result concluded by Banasiak et al. [38] experimentally demonstrated that the ejector efficiency of 0.3 could be achieved for an individual ejector hosted in a multi-ejector pack concerning the pressure lift and other inlet flow conditions. The current ejector cartridge efficiency was reasonably consistent with the results reported by Banasiak et al. [16], who registered a similar efficiency range when testing four different ejector cartridges. Furthermore, Fredslund et al. [39] obtained field data from installations placed in various places. The results observed vapor ejector efficiencies above 0.25 measured in the laboratory at typical operating conditions (P_{lift}=6 bar). Boccardi et al. [27, 40] evaluated a multi-ejector expansion pack having four different ejector geometries with motive nozzle throat diameters from 0.7 mm (similar to the current work) to 2.0 mm. The result revealed a maximum ejector efficiency, calculated by equation (3), of 0.18 due to the module's design for high pressure lift and low ER. Lucas et al. [12] recorded a maximum ejector efficiency of 0.22 in the experimental investigation using 0.62 mm throat diameter of driving nozzle at variant operation conditions. The authors stated that the pressure losses within the mixing chamber would be the more pronounced dependence of ejector efficiency. Despite all attempts to control the ejector discharged pressure to recover the expansion work effectively by regulating the motive nozzle geometries, controlling the mixer/diffuser geometries

would be a challenging investigation to reach higher efficiency in the future. Moreover, Haida et al. [41] and Banasiak et al. [42] managed to reach high efficiency up to 0.33 based on their different geometries and operating conditions for R744 systems even though higher ejector efficiency were published for other system using different working fluid than CO_2 [43]. Thus, to equip the ejector in an ideal way, the ejector pressure lift should be better adjusted according to the gas cooler heat sink conditions. Hence, the overall system performance will be maximized.

In such an analysis, it is not easy to represent the performance map of the ejector because the SN mass flow rate is a function of many derivative parameters such as entrainment ratio, work recovery rate, and ejector efficiency. However, Fig. 7 introduces the mass entrainment ratio characteristics at different receiver pressure. The analysis was performed at different motive nozzle flow pressure and temperature concerning two different evaporation temperatures, mainly -6°C and -3°C (approximately P_{SN}= 29.5 and 32 bar). The results expose the expected outcome based on the ejector theory principles. The pressure lift is observed to have an inverse proportional to the ejector mass entrainment ratio, at which increasing the receiver pressure for higher P_{lift} causes the mass entrainment ratio to drop sharply. This can be clarified by the working region mode of the ejector. For instance, when the receiver pressure is increasing, the shock waves will move closer to the region where the mixing process occurs and disturb the mixing. As a result, the suction nozzle flow stream will no longer be choked in the mixing chamber. Thus, less amount of SN fluid is drawn, and the mass entrainment ratio decreases further [44]. Fig. 7(a) illustrates the effect of different MN pressure on the ejector as the required amount of energy needed to accelerate and suck the SN flow by transforming the pressure energy of the motive flow into kinetic energy while mixing. Therefore, the mass entrainment ratio was predicted over several receiver pressure range. At double choking mode, when the MN pressure is increasing at constant MN temperature (T_{MN}= 20°C), the ejector will work at lower ER and operate at higher critical pressure (the exit pressure where the double choking mode ends). The reason associated with the increase of motive nozzle mass flowrate and aid to enlarge the expansion angle at the motive nozzle exit flow jet causing a reduction of the ejector annular effective area (area formed by the primary jet core and the mixing chamber wall where the suction fluid flow is choked) and increasing the resulting momentum of the mixed stream due to the higher velocity of the entrained stream attained. Therefore, the shockwaves will move downstream with a high compression ratio and pressure lift. On the other hand, if both motive and suction nozzle flow pressure and temperature will remain constant with increasing the receiver pressure, then the mass entrainment ratio will remain constant as represented in Fig. 7(a) at the critical mode only for the case at P_{MN}= 100 bar and P_{rec} from the range of 30.5 to 31.18 bar within ER = 0.7. Conversely, when the ejector operates at a single choking mode, increasing the motive nozzle flow pressure at fixed T_{MN} will decrease the entrainment ratio at a higher receiver pressure range. This reduction will characterize a slope steeper at lower motive

nozzle flow pressure. Related to the author's knowledge, most of the vapor compression CO_2 ejectors are working at subcritical mode. The figure also illustrates the possible receiver pressure working range at each motive nozzle pressure. For example, at T_{evap}= -6°C the ejector could work till P_{rec}= 34.6, 35.2, 36.6, 38, and 38.5 bar at P_{MN}= 60, 70, 80, 90 and 100 bar respectively. Besides, at T_{evap}= -3°C as shown in Fig. 7(b), the receiver working range will shift to start at P_{rec}= 33 bar. When the system is working at a relatively higher evaporation temperature, then the suction nozzle flow pressure will increase and at fixed motive flow conditions, the ejector will produce a higher entrainment ratio. This comes at a sacrifice of ejector pressure lift as can be seen in Fig. 7(b), where the highest possible P_{lift}= 6.51 at and T_{evap}= -3°C comparing with 9.18 bar at T_{evap}= -6°C. For example, at P_{MN}= 60 bar and P_{rec}= 33.5 bar, the mass entrainment ratio increased from 0.248 to 0.809 while P_{lift} dropped from 3.96 to 0.891 bar within increasing T_{evap} from -6 to -3°C. Likewise, at P_{MN}=80 bar and P_{rec}=32.9 bar, ER increased by 39% with 2.72 bar declined. Overall, higher T_{evap} served for higher ejector mass entrainment ratio, while lower evaporation temperature for freezing and cooling applications will provide a high ejector P_{lift} and compression ratio.

To find out the optimum motive nozzle flow condition, one can compare with the highest entrained suction nozzle flow at the widening range of receiver pressure, high ejector efficiency, and great P_{lift} could be gained. Among the different inlet motive nozzle flow pressures, 90 bar provided the maximum ejector performance based on the high efficiency and pressure lift comparatively. It is worth mentioning that CO_2 has a rather small difference of P_{rec} working range (determined as the ejector back pressure) as observed in the figures, downward trends steeper due to the low compression ratio of the R744 compared to other refrigerants [45]. In the same context, Fig. 7 (c and d) show the effect of the motive nozzle flow temperature on the ejector performance considering a fixed P_{MN} at 90 bar as an optimal motive pressure as well as to express the transcritical and subcooled test regions. The result revealed that the mass entrainment ratio is decreasing with decreasing motive nozzle flow temperatures. Despite having a higher pressure lift, the receiver pressure working range becomes much smaller for a higher motive nozzle flow temperature and then the mass entrainment ratio drops steeply. However, at the higher region of P_{rec}, the mass entrainment ratio behaved the same, and motive nozzle flow temperature does not play a crucial role in controlling the mass entrainment ratio. In contrast, at low receiver pressure, the attitudes are contradictory. For example, roughly at P_{rec} equal to 37.5 bar, ER = 0.227 and 0.167 for 35°C and 20°C motive nozzle flow temperature respectively, while when reducing the pressure 5 bar, then the mass entrainment ratio will increase to 0.590 and 0.984 accordingly. In the standard booster systems with target size from 40 to 150 kW, this result from low-pressure type ejectors is required to guarantee high suction mass flow, for instance, high mass entrainment ratio with reasonable pressure lift which is suitable for applications north in Europe where the climate is rather moderate and mild,

and little flash gas is formed depending on the ambient conditions [46]. Linking with higher evaporative temperature as demonstrated in Fig. 7(d), the ejector is shifting to work under higher receiver pressure with further steeper mass entrainment ratio. For instance, the ejector is working under the receiver pressure from 32.4 to 40 bar reaching a maximum mass entrainment ratio of 1.10. It should be emphasized that the mass entrainment ratio in the traditional ejector cooling system is relatively low compared with the two-phase CO_2 ejector.
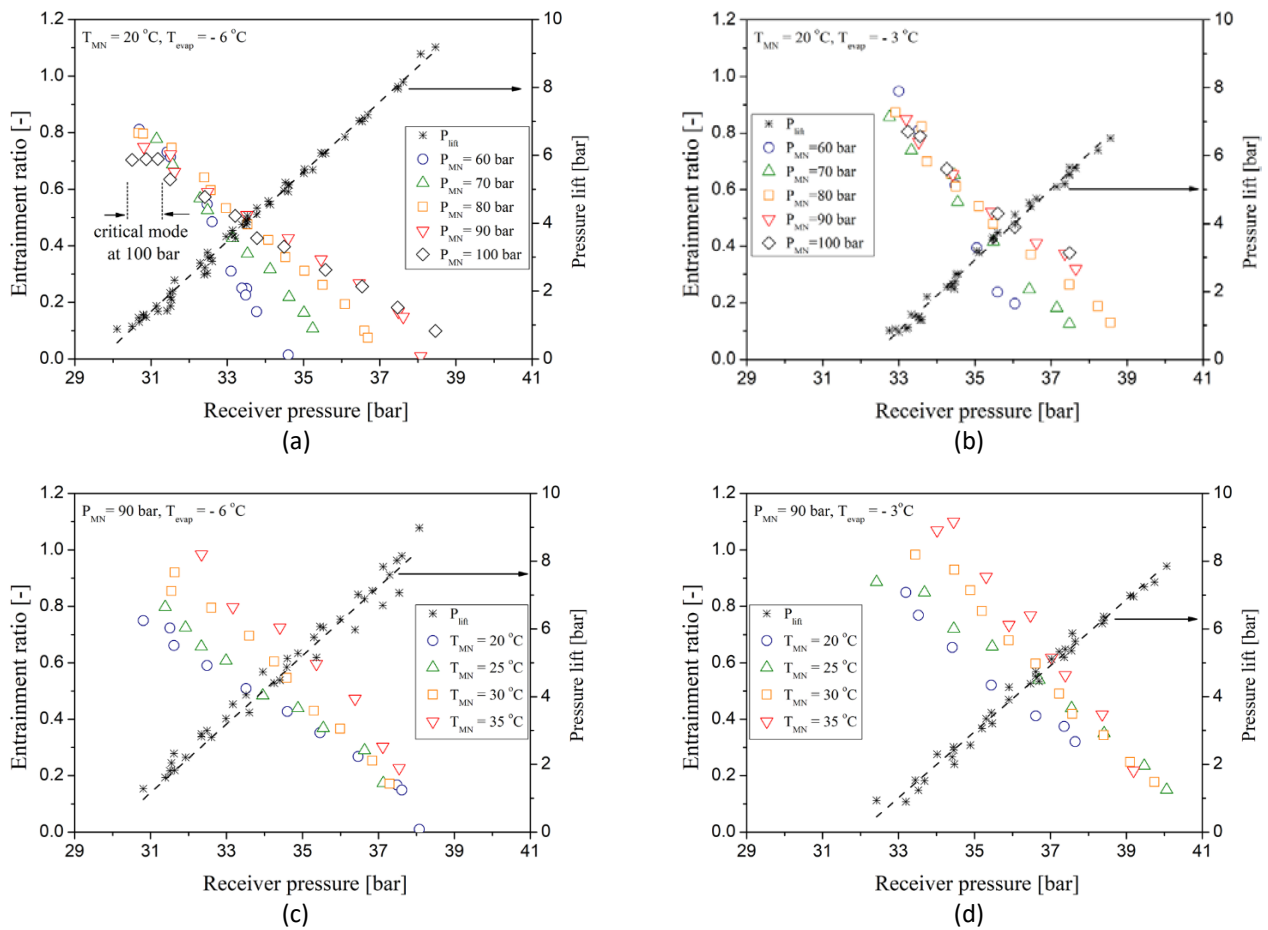

Figure 7: variation of ejector entrainment ratio with receiver pressure and P_{lift} as a function of motive flow conditions.

5.2. Effect of ejector on the system performance

In the transcritical R744 refrigeration systems, one of the improvement areas is the use of ejector-based expansion work recovery. The aforementioned result illustrated the effect of different boundary conditions on the ejector performance system. However, to achieve optimum energy efficiency, it is essential to control the exit gas cooler pressure precisely to maintain an efficient expansion work recovery with respect to the receiver pressure. The work recovery rate can be interpreted as the power used to compress the suction nozzle flow from the suction nozzle inlet to the ejector outlet

isentropically. Fig. 8 presents the ejector work recovery rate vs. receiver pressure at T_{MN}= 20°C and T_{evap}= -6°C. The highest value of the ejector work recovery rate was recorded as 0.096 kW at P_{MN}=100 bar. It was recognized how the work recovery rate is increased when the motive nozzle flow pressure is raised at fixed suction nozzle flow conditions. For example, at the P_{rec}≈ 31.5 bar, $\dot{W}_{recv}$ was doubled from 0.034 kW at P_{MN}= 60 bar to 0.068 kW at P_{MN}= 90 bar. The reason behind this rise relies on the higher amount of energy from the motive flows jet stream (higher momentum due to the increase of the motive mass flow rate) that energizes the entrained flow stream to accelerate. The result also implied that at constant motive nozzle flow pressure, the work recovery rate increases with increasing the receiver pressure to the maximum at which further increase at receiver pressure causes the work recovery rate to decline. Based on the previous result from Fig. 7, a similar trend of work recovery rate will be predicted in case of running the ejector at higher evaporation temperature or suction nozzle flow pressure with shifting the outlet pressure at higher receiver pressure.
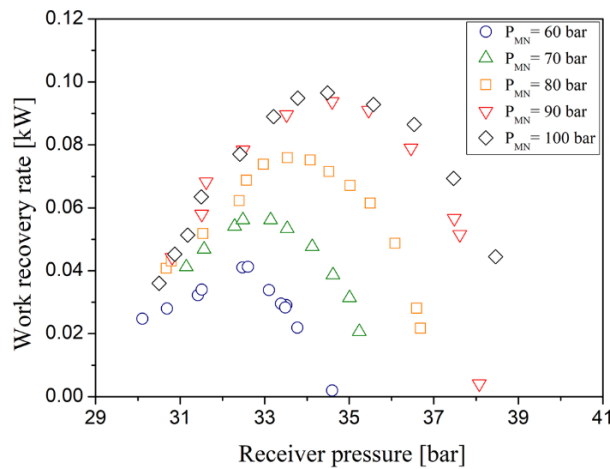

Figure 8: potential work recovery rate vs. receive pressure at T_{MN}=20°C, T_{evap}= -6°C

Based on equation (3), the experimental result was used to compare the ejector work rate recovery potential by the actual work rate recovery, as represented in Fig. 9. The constant lines of ejector efficiency for these measurement data are represented as well. The value demonstrated that the ejector achieved an efficiency of 1.8% to 35%. The data markers on the figure were taken at different outlet gas cooler pressure. Overall, increasing the motive nozzle flow pressure has a positive effect on the ejector performance, indicating higher work rate recovery. It can be observed that higher motive nozzle flow pressure results in a high motive mass flow rate and generate more considerable pressure difference in the system, which contributes to improving the overall available work recovery potential $\dot{W}_{recv,max}$. In addition, increasing the motive nozzle flow pressure at constant inlet temperature leads to higher specific enthalpies at which greater kinetic energies could be extracted at the ejector. However, when motive nozzle flow pressure exceeding 90 bar, the maximum work recovery rate will continue to some extent increase with a slightly decreased in the maximum ejector efficiency,

which proves the capability of the ejector to provide adequate performance over a different range of operating conditions. Comparing with the common observed HFCs and HFOs refrigerants, CO_2 excess work recovery efficiency with 30% because it could overcome the significant pressure loss in the ejector due to higher vapor density [47].
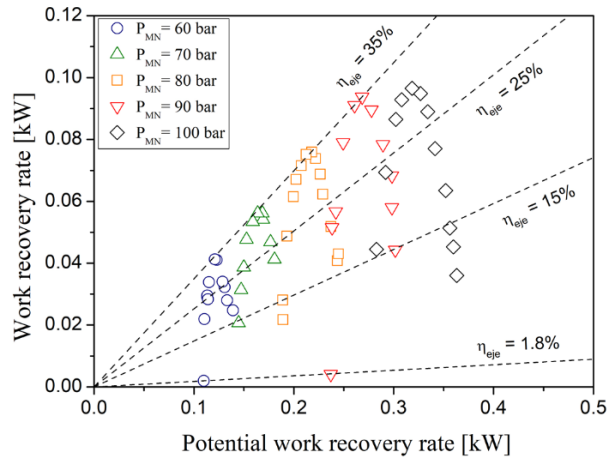

Figure 9: Experimental ejector efficiency for different motive nozzle flow pressure at T_{MN}=20°C, T_{evap}= -6°C.

Under different receiver and motive nozzle flow pressures, the ejector performance of the efficiency, work rate recovery, mass entrainment ratio, pressure lift, and the cooling system COP are analyzed and discussed. In Fig. 10, the analysis performed at P_{rec}= 34.6 bar, T_{MN}= 20°C and T_{evap}= -6°C via different motive nozzle flow pressure. The result indicates that the ejector efficiency was rising with increasing the motive nozzle flow pressure up to 90 bar where η_{eje}= 35% then start to decrease. As expected, having very high pressure will require more compressor power and lead to an increase in potential work recovery, and then the ejector work recovery starts to drop. This explains the reason for the COP reduction since the data represented at constant evaporation temperature. At the fixed receiver pressure, the pressure lift continued to remain at the range of 5 bar for these cases. The mass entrainment ratio was reported to be continuously increasing from 0.014 to 0.428 until the motive nozzle flow pressure reaches 90 bar, influenced by the rapid increase of the entrained mass flow comparing to the motive mass flow, then dropping down.

Fig. 11 shows the ejector performance data plotted at different receiver pressure. The experimental result obtained at a motive nozzle flow pressure of 90 bar as an optimal motive working pressure. The motive nozzle flow temperature sets at 20°C and the evaporation temperature equal to -6°C. Again, the pressure lift in the ejector cooling system is the desired benefit. With increasing the receiver pressure as the ejector mixed-flow outlet, the pressure lift will keep increasing linearly to the maximum of 8.99 bar at which P_{rec}= 38.1 bar. In contrast, the mass entrainment ratio is decreasing with increasing receiver pressure from 0.749 to 0.010, and a further increase in the receiver pressure will come at a sacrifice of the mass

entrainment ratio and cause an ejector malfunction where it works as an expansion valve for higher pressure lift. Therefore, the ejector suction port is occupied with the check valve to prevent backflow. In other words, the small mass entrainment ratio results in a large pressure lift at constant motive nozzle flow pressure. Based on this reverse proportionality between the pressure lift and the mass entrainment ratio, one should control the operation condition of the ejector for the optimum performance. This should be evaluated at the highest work recovery rate and ejector efficiency of 34.95%. Therefore, the receiver pressure was selected to be 34.6 bar. The cooling COP of the system remains almost unchanged at 2.59 because the compressor power is fixed for constant gas cooler pressure and the cooling load.
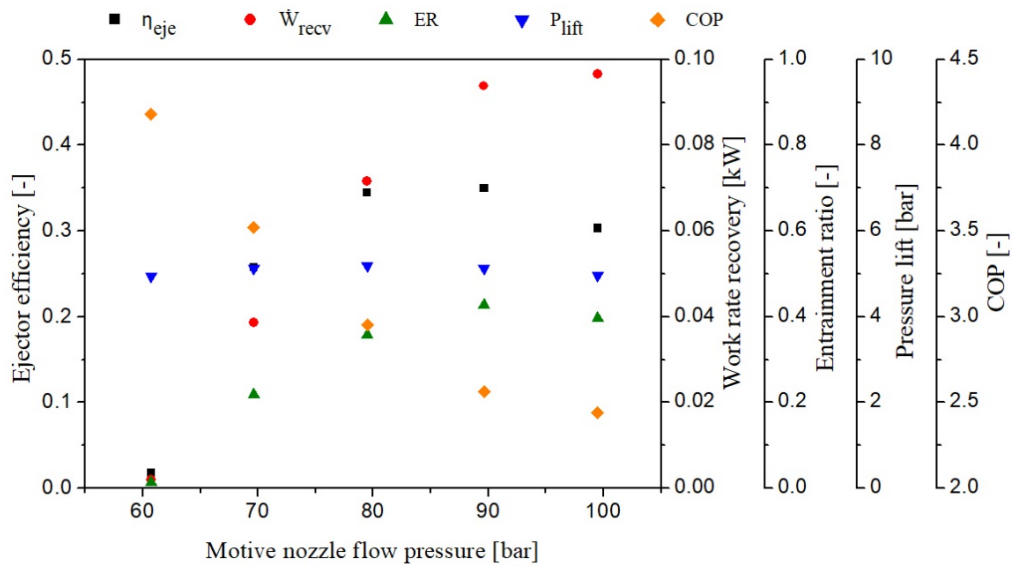

Figure 10: Cooling COP, η_{eje}, P_{lift}, $\dot{W}_{recv}$, and ER vs. different P_{MN} at P_{rec}= 34.6 bar, T_{MN}= 20°C and T_{evap}= -6°C.

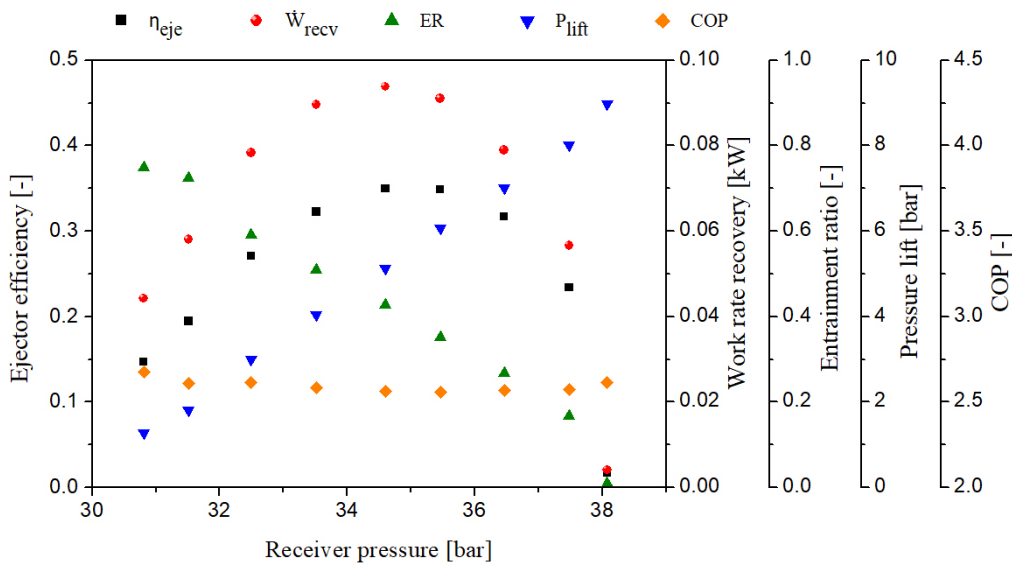
Figure 11: Cooling COP, η_{eje}, P_{lift}, $\dot{W}_{recv}$, and ER vs. different P_{rec} at P_{MN}= 90 bar, T_{MN}= 20°C and T_{evap}= -6°C.

5.3. Exergy analysis result

The exergy efficiencies and irreversibility in the ejector are determined based on the exergy transit analysis for different operation conditions. The comparison analysis of exergy produced, exergy consumed, and exergy destruction was evaluated in terms of different motive flow and receiver pressure based on the experimental results. In Fig. 12(a), the variation of the transiting ejector exergy efficiencies and exergy destruction at T_{MN}=20°C, T_{evap}= -6°C for different motive nozzle flow pressure are represented via different receiver pressure. When the receiver pressure increased, the ejector exergy efficiency was rising to a certain level where it reaches the maximum then witness a decrease with any further receiver pressure rise. There existed a maximum exergy efficiency of 17.9% at corresponding P_{MN}= 90 bar, which grows as the optimum exergy efficiency from 14.9% at P_{MN}= 60 bar then declines to 15.6% with increasing the motive nozzle flow pressure to 100 bar. Nonetheless, the exergy destruction was increasing with higher motive nozzle flow pressure. The maximum loss was 0.98 kW at P_{MN}= 100 bar, while the minimum took place at P_{MN}= 60 bar with 0.4 kW inside this two-phase ejector. It may be observed that the total exergy destruction increased by about 17% when increasing the motive nozzle flow pressure from 90 to 100 bar. Based on that, the result nominated P_{MN}= 90 bar as the optimal gas cooler pressure, which agrees with the previous section analysis. Therefore, a comparison of different evaporation temperatures as well as outlet gas coolers was investigated under 90 bar of motive nozzle flow pressure. Fig. 12(b) represents the influence of different motive nozzle flow temperatures on the ejector exergy efficiency and destruction at P_{MN}= 90 bar and T_{evap}= -6°C. It can be noted that regardless of the receiver pressure, working at higher exit gas cooler temperatures will increase the exergy efficiency and decrease the loss of the exergy significantly. The reason lies in the lower exergy consumed associated with low inlet mass flow rate through the ejector. For instance, at T_{MN}= 20°C and receiver pressure around 34.5 bar, the maximum exergy efficiency recorded was 17.9%, with 0.619 kW exergy destruction. This loss will shrink to 32% lower in the case of working under a motive nozzle flow temperature of 35°C and raise the exergy efficiency to 23%. Moreover, the experimental data did not illustrate much performance improvement when increasing the motive nozzle flow temperature from 20°C to 25°C and showed somewhat similar exergy destruction. As a result, working at a supercritical motive flow region will allow the ejector to avoid the massive amount of exergy destruction and expressively increase the exergy efficiency. For the sake of introducing the optimum motive flow working condition, the exergy analyses should be represented. Fig. 13 showed the characteristic of the ejector under different motive nozzle flow temperature and pressure. Fig. 13(a) analysed the data at P_{rec}≈35.4, T_{evap}= -6°C and P_{MN}= 34.5 bar whiles Fig. 13(b) assessed the result at P_{rec}≈34.6 bar, T_{evap}= -6°C and T_{MN}= 20°C. It could be noted that the ejector performed higher exergy efficiency in case of running at T_{MN}= 35°C by 22.3% and lower the exergy consumed and destruction gradually while the total exergy production

remained level at approximately 0.124 kW through the motive temperature increase. The exergy efficiency slowly grew when T_{MN} raised from 20°C to 25°C as were discussed previously, then strikingly increased.
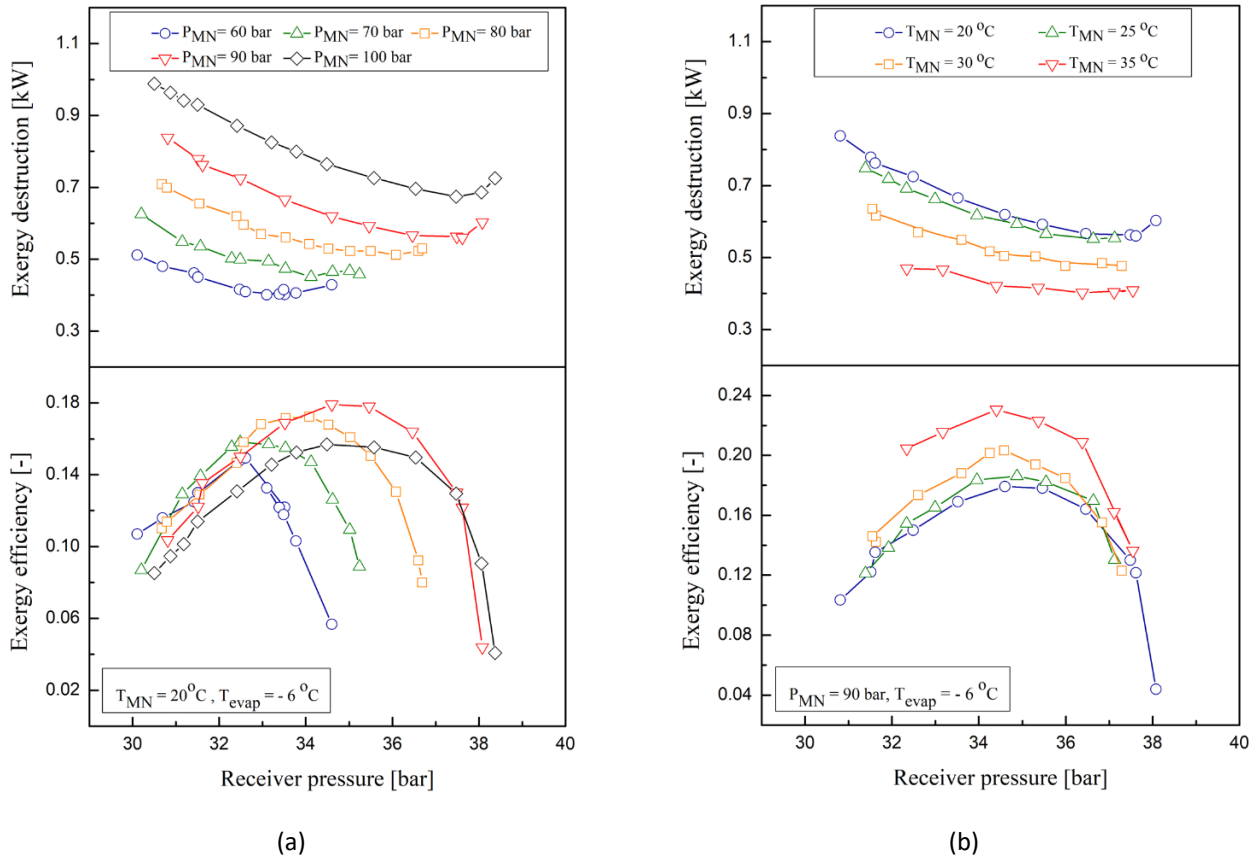

(a)   (b)

Figure 12: Ejector exergy efficiency and destruction vs. P_{rec}, (a) at different motive pressure, (b) at different motive temperatures.

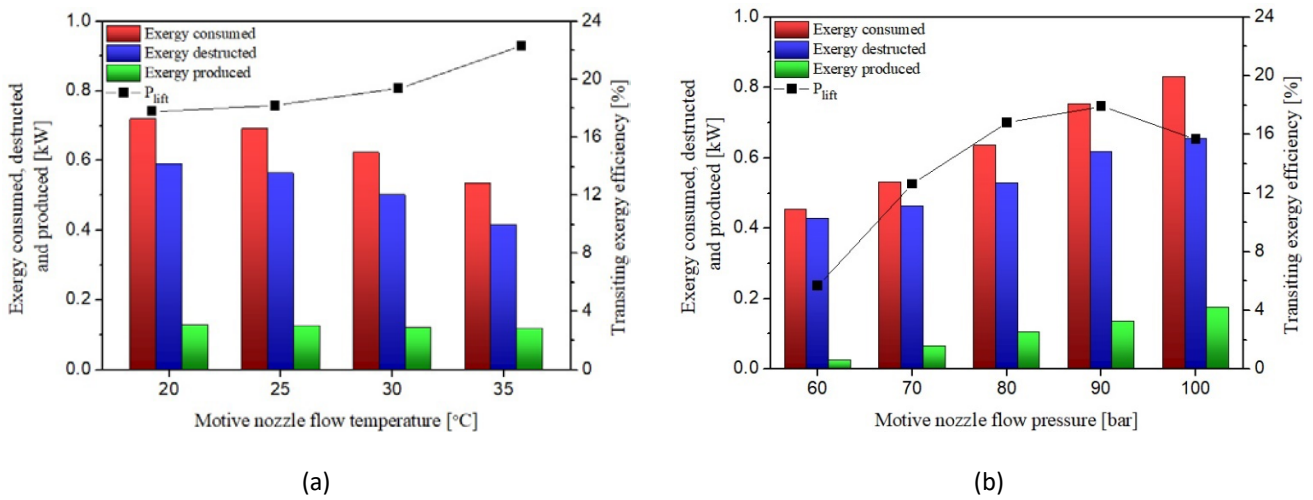(a)   (b)

Figure 13: Ejector exergy metrics at different motive nozzle flow temperatures and pressure at T_{evap}= -6°C, (a) P_{rec}≈ 35.4 bar and P_{MN}= 34.5 bar, (b) P_{rec}≈ 34.6 bar and T_{MN}= 20°C.

In Fig. 13(b), the highest exergy efficiency recorded at P_{MN}= 90 bar by dramatically increase from 5.67% at P_{MN}= 60 bar to 17.92% then declines noticeably. In contrast, the amount of the exergy consumed and destruction were increased progressively with higher motive nozzle flow pressure while the exergy produced growing from 0.026 kW at P_{MN}= 60 bar to 0.142 kW at P_{MN}= 90 bar then remained level with further pressure increased. All behaviour of the thermodynamic metrics, including exergy consumed as the feeding exergy $\nabla \dot{E}_{tr}$, exergy produced as the useful exergy product $\Delta \dot{E}_{tr}$, the exergy destruction, transiting inlet and outlet exergy are represented in Table 3 at P_{MN}= 90 bar and T_{MN}= 35°C over various receiver pressure. These conditions were specified based on the optimal motive nozzle flow pressure and temperature represented in the previous part discussion.

Table 3.

Exergy metrics of the experiment for different evaporation temperature and receiver pressure.

T_{evap} [°C]	P_{rec} [bar]	Exergy Consumed [kW]	Exergy Produced [kW]	Exergy Destruction [kW]	Transiting Exergy [kW]	Exergy Efficiency %	Inlet Exergy [kW]	Outlet Exergy [kW]
-6	32.34	0.590	0.121	0.470	7.765	20.44	8.355	7.886
-6	33.17	0.595	0.128	0.466	7.354	21.58	7.949	7.482
-6	34.40	0.547	0.126	0.421	6.889	23.06	7.436	7.015
-6	35.37	0.535	0.119	0.416	6.554	22.30	7.090	6.674
-6	36.38	0.509	0.106	0.402	5.985	20.89	6.494	6.092
-6	37.11	0.482	0.078	0.404	5.254	16.19	5.735	5.332
-6	37.55	0.473	0.064	0.409	4.958	13.62	5.431	5.023
-3	34.45	0.544	0.090	0.453	8.380	16.60	8.923	8.470
-3	35.31	0.544	0.102	0.441	7.956	18.85	8.500	8.059
-3	35.91	0.530	0.108	0.423	7.307	20.32	7.837	7.414
-3	36.47	0.486	0.107	0.379	7.048	22.04	7.533	7.155
-3	37.39	0.470	0.099	0.370	6.323	21.12	6.792	6.422
-3	38.36	0.442	0.085	0.357	5.640	19.27	6.083	5.726
-3	39.19	0.427	0.058	0.369	4.904	13.64	5.331	4.962

The analysis evaluated the ejector at different evaporation pressure to study the effect of the suction nozzle flow parameters. In general, working under low evaporation temperature is required to discharge more heat load from the system at the gas cooler and has a direct impact on the compressor capacity. Also, at lower evaporation temperature, the ejector suction pressure will decrease and reduce the suction mass flow rate. Therefore, at the same motive flow condition, the total exergy consumed will be higher. It can be noted that the exergy consumed and destructed, as well as the transiting exergy, were decreasing with increasing the receiver pressure. The maximum exergy consumed at T_{evap}= -6°C equals to 0.595 kW, which is 8.6% higher than the maximum exergy consumed in case of running at T_{evap}= -3°C. The result indicated

excessively exergy destruction compare to the useful one. According to the data characterized in the table, the exergy produced represent 13.6% to 23% of the total exergy consumed. The most exergy losses took place at higher receiver pressure equipped with low ejector exergy efficiency. In that respect, working at T_{evap}= -3°C could minimize the exergy destruction due to lower total exergy consumed but account for a slightly lower efficiency working region. One can observe the slow increase of the transiting exergy efficiency by 3% at T_{evap}= -6°C and 5% at T_{evap}= -3°C with higher receiver pressure to 23% an 22% respectively, then decreased for both of them to 14%. However, both inlet and outlet exergy represent an increase with increasing the evaporator temperature and decline with increasing the receiver pressure based on the presence of transiting exergy. Because of high ejector exergy destruction, computational fluid dynamics will be performed later on this ejector to predict all the component exergy loss and probe the physical insight of the ejector.

6. Conclusion

The paper investigated a detailed experimental work and exergy analysis on the R744 transcritical ejector cooling system. The influence of different motive nozzle flow pressure and temperature, evaporation temperature, and ejector outlet flow represented in the receiver pressure on the ejector performance were evaluated. In order to ensure a stable load at the heat exchangers, the coefficient of liquid mass balance was calculated to guarantee that all the experimental data collected at the steady-state conditions. Finding the optimum working range of the ejector is necessary for an efficient R744 system. Therefore, the ejector operating parameters such as pressure lift, mass entrainment ratio, work rate recovery and efficiency were evaluated. The main findings can be summarized as follows:

(1) The tested ejector could provide a maximum pressure lift of 9.51 bar which could be defined in a linear relation with the motive nozzle flow pressure. This correlation helps in controlling the parallel compressor pressure ratio and contributes to improve the system performance.

(2) The results indicated that increasing the evaporation temperature influence the ejector pressure lift by decreasing and holding up the inverse proportional with the mass entrainment ratio. Additionally, with higher evaporative temperature, the ejector is shifting to work under higher receiver pressure with further steeper mass entrainment ratio whiles increasing the motive nozzle flow pressure allows stretching the ejector receiver pressure working rang.

(3) Among different exit gas cooler conditions, the ejector was able to recover up to 36.9% of the throttling losses according to the efficiency metric definition.

(4) With respect to the motive nozzle flow pressure, the results revealed a better overall performance when the ejector operated at supercritical conditions relatively at 90 bar. It was found that the ejector was working at subcritical mode (single choking) in most of the cases and the receiver pressure range was very short (less than 10 bar) comparing to other refrigerants.

(5) Based on the exergy distribution findings, the ejector holds high exergy efficiency when working at higher exit gas cooler temperatures along with providing lower exergy destruction. The amount of the exergy consumed and destruction proved to be increasing progressively with higher motive nozzle flow pressure while in contrast, decreasing with higher motive nozzle flow temperature.

Finally, it is worth highlighting that the obtained results could provide a useful aid for researchers and designers to select the best working region of the ejector by setting up the optimal operating variables. As future work, a specific investigation on the numerical modelling will be devoted to this ejector to capture the local behaviour of this complex two-phase flow.

References

[1]   Alberto Cavallini and Claudio Zilio. Carbon dioxide as a natural refrigerant. International Journal of Low-Carbon Technologies, 2(3):225–249, 2007.

[2]   Michal Haida, Jacek Smolka, Michal Palacz, Jakub Bodys, Andrzej J Nowak, Zbigniew Bulinski, Adam Fic, Krzysztof Banasiak, and Armin Hafner. Numerical investigation of an r744 liquid ejector for supermarket refrigeration systems. Thermal Science, 20(4):1259–1269, 2016.

[3]   I-p Edition. 2009 ASHRAE Handbook - Fundamentals (SI Edition). American Society of Heating, Refrigerating and Air-Conditioning Engineers, Inc., 2009.

[4]   Paride Gullo, Armin Hafner, Krzysztof Banasiak, Silvia Minetto, and Ekaterini E Kriezi. Multi-ejector concept: A comprehensive review on its latest technological developments. Energies, 12(3):406, 2019.

[5]   J.S.H. Carbon dioxide as a refrigerant. Journal of the Franklin Institute, 196(5):713, 1923.

[6]   Farivar Fazelpour and Tatiana Morosuk. Exergoeconomic analysis of carbon dioxide transcritical refrigeration machines. International journal of refrigeration, 38:128–139, 2014.

[7]   Stefan Elbel and Neal Lawrence. Review of recent developments in advanced ejector technology. International Journal of Refrigeration, 62:1–18,2016.

[8]   Stefan Elbel and Pega Hrnjak. Flash gas bypass for improving the performance of transcritical r744 systems that use microchannel evaporators. International Journal of Refrigeration, 27(7):724–735, 2004.

[9]   Giorgio Besagni, Riccardo Mereu, and Fabio Inzoli. Ejector refrigeration: a comprehensive review. Renewable and Sustainable Energy Reviews, 53:373–407, 2016.

[10]   Michal Haida, Jacek Smolka, Armin Hafner, Ziemowit Ostrowski, Michał Palacz, Kenneth B Madsen, Sven Försterling, Andrzej J Nowak, and Krzysztof Banasiak. Performance mapping of the r744 ejectors for refrigeration and air conditioning supermarket application: A hybrid reduced-order model. Energy, 153:933–948, 2018.

[11]   Stefan Elbel. Historical and present developments of ejector refrigeration systems with emphasis on transcritical carbon dioxide air-conditioning applications. International Journal of Refrigeration, 34(7):1545–1561, 2011.

[12]   Christian Lucas and Juergen Koehler. Experimental investigation of the cop improvement of a refrigeration cycle by use of an ejector. International Journal of Refrigeration, 35(6):1595–1603, 2012.

[13]   Yang He, Jianqiang Deng, Lixing Zheng, and Zaoxiao Zhang. Performance optimization of a transcritical CO_2 refrigeration system using a controlled ejector. International Journal of Refrigeration, 75:250–261, 2017.

[14]   Yang He, Jianqiang Deng, Fusheng Yang, and Zaoxiao Zhang. An optimal multivariable controller for transcritical CO_2 refrigeration cycle with an adjustable ejector. Energy Conversion and Management, 142:466–476, 2017.

[15]   Armin Hafner, Sven Försterling, and Krzysztof Banasiak. Multi-ejector concept for r-744 supermarket refrigeration. International Journal of Refrigeration, 43:1–13, 2014.

[16]   Krzysztof Banasiak, Armin Hafner, Ekaterini E Kriezi, Kenneth B Madsen, Michael Birkelund, Kristian Fredslund, and Rickard Olsson. Development and performance mapping of a multi-ejector expansion work recovery pack for r744 vapour compression units. International Journal of Refrigeration, 57:265–276, 2015.

[17]   Zhe Chen, Nan Guo, and Robert C Qiu. Demonstration of real-time spectrum sensing for cognitive radio. IEEE Communications Letters, 14(10):915–917, 2010.

[18]   Ivan Najdenov, Karlo T Raić, and Gordana Kokeza. Aspects of energy reduction by autogenous copper production in the copper smelting plant bor. Energy, 43(1):376–384, 2012.

[19]   Jacek Smolka, Michal Palacz, Jakub Bodys, Krzysztof Banasiak, Adam Fic, Zbigniew Bulinski, Andrzej J Nowak, and Armin Hafner. Performance comparison of fixed-and controllable-geometry ejectors in a CO_2 refrigeration system. International Journal of Refrigeration, 65:172–182, 2016.

[20]   Michal Palacz, Jacek Smolka, Andrzej J Nowak, Krzysztof Banasiak, and Armin Hafner. Shape optimisation of a two-phase ejector for CO_2 refrigeration systems. International Journal of Refrigeration, 74:212–223, 2017.

[21]   Fang Liu, Eckhard A Groll, and Daqing Li. Modeling study of an ejector expansion residential CO_2 air conditioning system. Energy and buildings, 53:127–136, 2012.

[22]   Stefan Elbel and Pega Hrnjak. Experimental validation of a prototype ejector designed to reduce throttling losses encountered in transcritical r744system operation. International Journal of Refrigeration, 31(3):411–422, 2008.

[23]   M Nakagawa, AR Marasigan, T Matsukawa, and A Kurashina. Experimental investigation on the effect of mixing length on the performance of two-phase ejector for CO_2 refrigeration cycle with and without heat exchanger. International Journal of Refrigeration, 34(7):1604–1613, 2011.

[24]   Sahar Taslimi Taleghani, Mikhail Sorin, and Sébastien Poncet. Analysis and optimization of exergy flows inside a transcritical CO_2 ejector for refrigeration, air conditioning and heat pump cycles. Energies, 12(9):1686, 2019.

[25]   Paride Gullo, Armin Hafner, and Krzysztof Banasiak. Thermodynamic performance investigation of commercial r744 booster refrigeration plants based on advanced exergy analysis. Energies, 12(3):354, 2019.

[26]   Tao Bai, Jianlin Yu, and Gang Yan. Advanced exergy analyses of an ejector expansion transcritical CO_2 refrigeration system. Energy Conversion and Management, 126:850–861, 2016.

[27]   G Boccardi, F Botticella, G Lillo, R Mastrullo, AW Mauro, and R Trinchieri. Thermodynamic analysis of a multi-ejector, CO_2, air-to-water heat pump system. Energy Procedia, 101:846–853, 2016.

[28]   H Kursad Ersoy and Nagihan Bilir. Performance characteristics of ejector expander transcritical CO_2 refrigeration cycle. Proceedings of the Institution of Mechanical Engineers, Part A: Journal of Power and Energy, 226(5):623–635, 2012.

[29]   S Taslimi Taleghani, M Sorin, and S Poncet. Energy and exergy efficiencies of different configurations of the ejector- based refrigeration systems CO_2. Towards Energy Sustainability, page 99, 2018.

[30]   Sun Fangtian and Ma Yitai. Thermodynamic analysis of transcritical CO_2 refrigeration cycle with an ejector. Applied Thermal Engineering, 31(6-7):1184–1189, 2011.

[31]   Danfoss. How to design a transcritical CO_2 system Type CTM 6 High Pressure (HP) and Low Pressure (LP). 2018.

[32]   Anas F A Elbarghthi, Saleh Mohamed, Van Vu Nguyen, Vaclav Dvorak, et al. CFD based design for ejector cooling system using HFOs (1234ze (e) and1234yf). Energies, 13(6):1408, 2020.

[33]   JCGM/WG. Evaluation of Measurement Data, Guide to the expression of uncertainty in measurement. International Organization for Standardization Geneva ISBN, 50(September):134, 2008.

[34]   Krzysztof Banasiak, Michał Palacz, Armin Hafner, Zbigniew Buliński, Jacek Smołka, Andrzej J Nowak, and Adam Fic. A CFD-based investigation of the energy performance of two-phase r744 ejectors to recover the expansion work in refrigeration systems: an irreversibility analysis. International journal of refrigeration, 40:328–337, 2014.

[35]   Vadim M Brodyansky, Mikhaïl V Sorin, and Pierre Le Goff. The efficiency of industrial processes: exergy analysis and optimization, volume 9. Elsevier Amsterdam, 1994.

[36]   Marc A. Rosen and Ibrahim Dincer. Effect of varying dead-state properties on energy and exergy analyses of thermal systems. International Journal of Thermal Sciences, 43(2):121–133, 2004.

[37]   Yinhai Zhu, Conghui Li, Fuzhen Zhang, and Pei-Xue Jiang. Comprehensive experimental study on a transcritical CO_2 ejector expansion refrigeration system. Energy Conversion and Management, 151:98–106, 2017.

[38]   K Banasiak, A Hafner, O Haddal, and T Eikevik. Test facility for a multiejector r744 refrigeration system. In Proceedings of the 11th IIR Gustav Lorentzen Conference on Natural Refrigerants, Hangzhou, China, volume 31, 2014.

[39]   K Fredslund, EE Kriezi, KB Madsen, M Birkelund, and R Olsson. CO_2 installations with a multi ejector for supermarkets, case studies from various locations. In Proceedings of the 12th IIR Gustav Lorentzen Natural Working Fluids Conference, Edinburgh, UK, pages 21–24, 2016.

[40]   G Boccardi, F Botticella, G Lillo, R Mastrullo, AW Mauro, and R Trinchieri. Experimental investigation on the performance of a transcritical CO_2 heat pump with multi-ejector expansion system. International Journal of Refrigeration, 82:389–400, 2017.

[41]   Michal Haida, Krzysztof Banasiak, Jacek Smolka, Armin Hafner, and Trygve M Eikevik. Experimental analysis of the r744 vapour compression rack equipped with the multi-ejector expansion work recovery module. International journal of refrigeration, 64:93–107, 2016.

[42]   Krzysztof Banasiak, Armin Hafner, and Trond Andresen. Experimental and numerical investigation of the influence of the two-phase ejector geometry on the performance of the r744 heat pump. International journal of Refrigeration, 35(6):1617–1625, 2012.

[43]   N Bilir Sag, HK Ersoy, A Hepbasli, and HS Halkaci. Energetic and exergetic comparison of basic and ejector expander refrigeration systems operating under the same external conditions and cooling capacities. Energy conversion and management, 90:184–194, 2015.

[44]   Natthawut Ruangtrakoon, Tongchana Thongtip, Satha Aphornratana, and Thanarath Sriveerakul. CFD simulation on the effect of primary nozzle geometries for a steam ejector in refrigeration cycle. International Journal of Thermal Sciences, 63:133–145, 2013.

[45]   S Taslimi Taleghani, M Sorin, and S Poncet. Modeling of two-phase transcritical CO_2 ejectors for on-design and off-design conditions. International Journal of Refrigeration, 87:91–105, 2018.

[46]   Bajja Hamza. Experimental analysis of r744 multi-ejector modules. Norwegian University of Science and Technology, pages 154, 2019.

[47]   Neal Lawrence and Stefan Elbel. Experimental investigation of a two-phase ejector cycle suitable for use with low-pressure refrigerants r134a andr1234yf. International Journal of Refrigeration, 38:310–322, 2014.